

High performace tapped-inductor buck driver for LED arrays

M. APETREI*, A. GEORGESCU^a

Department of Physics, "Ovidius" University of Constanta, Constanta, 900527, Romania

^aSchool of Engineering and Computing Sciences, Texas A&M University of Corpus Christi, Corpus Christi, 78412, Texas, United States of America

Over the last years there has been a constant increase in the number of Light Emitting Diodes (LED) applications because of their small size and high luminous efficacy. In order to fully benefit from the improvements in LED technology, the driver also plays an important role in the total system efficacy. The present paper covers the design, fabrication and testing of a high efficiency 30W tapped-inductor buck converter especially suited for use in luminaires employing LED arrays.

(Received July 6, 2013; accepted May 7, 2015)

Keywords: LED, Array, Lighting, Driver, Tapped, Buck, Converter, Efficiency, Luminaire

1. Introduction

These days a big trend in lighting is with LEDs because of their small weight, low power consumption and cool operating temperatures. High power, high brightness LEDs are constantly evolving. Developments in the manufacturing technology have pushed the luminous efficacy far beyond the 100lm/W boundary [1, 2]. Before too long, it seems 200lm/W will become the benchmark of excellence that 100 lm/W is today as Phillips announced [3]. It is predicted that over the next years the use of LEDs in the lighting and consumer sectors will continue to grow dramatically [4]. With the introduction of multi-chip LED arrays the assembly cost has decreased, allowing luminaire manufacturers to provide high lumen output from compact light sources. Also the package thermal resistances are constantly being optimised for easier heatsink integration of high-power, high-brightness LEDs.

In order to benefit from these improvements in LED technology, the driver efficiency must also be maximized. Conventional Buck drivers operated of a high voltage input bus can provide high efficiency figures when the output voltage is also high [5] but show a declining efficiency when operated at high input/output voltage conversion ratios. LED arrays typically have a nominal voltage below 50V and the commonly used circuits attain efficiencies around 82 to 86% when used as LED array drivers.

By comparison the proposed circuit has a minimum efficiency of 90,2% and a peak efficiency of 93,8% with many 30W LED arrays. The goal of this project was attaining maximum conversion efficiency at a low cost and using widely available components. The only custom component is the tapped-inductor. The converter prototype has a small footprint and includes protections against overvoltage, output short-circuit and over-temperature,

providing a good reliability. Because of the high efficiency it does not require external heat sinks.

2. The proposed driver

Compared to conventional Buck converters, the tapped-inductor driver lowers the current stress on the main switch Q1 and the voltage stress on the catch diode D1 (Figure 1), allowing (in some cases) the replacement of the high voltage ultrafast catch diode with a Schottky one.

This increases the efficiency because the Schottky diode has a lower forward voltage drop and negligible reverse recovery switching losses. It also allows the use of a lower current main switch for lower cost and reduced switching losses. In the current implementation of the tapped inductor buck converter, the places of inductor L1a and main switch Q1 have been reversed to allow the addition of a lossless snubber (D2, D3, Cs), further improving efficiency by recycling the leakage inductance energy to the output of the converter.

The proposed circuit has a maximum output power of 30W and can also be used for powering a series string of high power LEDs provided that the string voltage and current needs are met.

The converter operates from a wide range, high voltage, direct current input bus which is assumed to be provided by a central power factor correction unit for the entire building to be illuminated [5]. The driver has an input voltage range between 250–420V and works in pulse-skipping mode.

The driver is flexible, allowing a range of output voltages ranging from 19V to 47V. The output current can be preset between 250mA and 700mA. Load current regulation is better than $\pm 0,6\%$ over the whole output voltage range and better than $\pm 4\%$ over the 0°C to 50°C ambient temperature range.

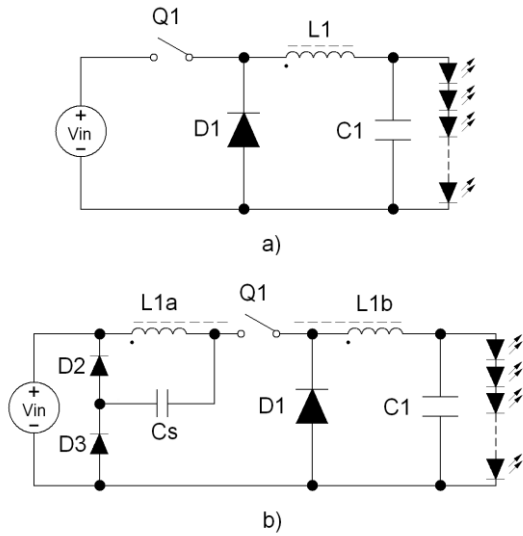


Fig. 1. Simplified schematics: a). Standard Buck driver;
b). Proposed tapped inductor driver

3. Circuit design

For the current project, we selected a TNY268GN integrated circuit based on cost, availability, integration and key parameters such as necessary peak current and various losses. The TinySwitch II chip family provides a high degree of integration in a small DIP7 package: a 700V low R_{DS-ON} MOSFET, a high voltage switched current source, oscillator, current limit and thermal shutdown functions.

The oscillator runs at 132 KHz and has its frequency dithered by ± 4 kHz. The modulation rate of the frequency jitter is set to 1 kHz to optimize EMI reduction for both average and quasi-peak emissions. This allows using a smaller input filter and reduces system cost. The current limiting circuit has a 215ns internal leading edge blanking interval. The thermal shutdown protects the circuit from overheating in case of an output short circuit or component failure. It activates at a typical temperature of 135°C with a hysteresis of 70°C. The integrated auto-restart circuit safely limits output power during fault conditions such as output short circuit or open loop [6].

Unlike conventional PWM (Pulse Width Modulation) controllers, the circuit operates in an ON/OFF fashion; it regulates output current by skipping switching cycles. This simplifies the driver schematic, eliminating control loop compensation components. It also improves efficiency at low output power, as by skipping cycles the MOSFET switching losses are reduced.

The circuit operates in the following manner: the internal clock of the TinySwitch-II runs all the time and the EN/UV input is sampled at the beginning of each clock cycle. If the current sunk out of the EN/UV pin is below 240 μ A the internal MOSFET commences a switching cycle that ends when the preset current limit or the maximum duty cycle is reached. When the current sunk out of the EN/UV pin is greater than 240 μ A, the internal

control circuitry generates a signal that turns OFF the power MOSFET for the entire switching cycle.

The internal state machine monitors the sequence of skipped pulses and lowers the current limit at light loads to prevent switching in the audible range and avoiding noises in the inductor.

At maximum load, TinySwitch-II will conduct during all of its clock cycles. At slightly lower load, it will “skip” additional cycles in order to maintain current regulation at the driver output. At medium loads, cycles will be skipped and the current limit will be reduced. At very light loads, the current limit will be reduced even further.

In this configuration, the output voltage ripple depends only on the output capacitor value, the switching energy and the delay of the feedback. The low impedance present at the EN/UV input pin optimizes optocoupler response time. As a result the response time is very fast, providing tighter regulation and better transient response compared to the performance of a PWM controller.

The tapped buck converter offers the advantage of reduced magnetic component size, reduced current stress on the main switch U1, and reduced voltage stress on the catch diode D3 (references Fig 3). The reduced current stress on the main switch means less switching loss and enables the use of a smaller device for a more cost effective design. The lower voltage stress on D3 enables the use of a low forward voltage Schottky diode for improved efficiency.

In order to fully exploit the power capability of the integrated power MOSFET, it is desirable to choose the power stage components such that at the minimum input voltage, maximum output voltage and maximum output power no switching cycles are skipped or terminated prematurely by the current limit circuitry assuming mostly discontinuous operation mode. The maximum duty cycle limit for TNY268 is guaranteed at 62% and the minimum current limit is 512mA. From this and the design parameters we can calculate the minimum inductance necessary to avoid premature current limiting:

$$L_{MIN} \geq \frac{V_{IN_MIN} - V_{OUT_MAX}}{I_{PK_MIN} * f_{SW_MIN}} * D_{MAX} \quad (1.1)$$

$$L_{MIN} \geq 1,96mH.$$

To avoid saturation due to integrated circuit current limit tolerance, this inductor will be selected to have a saturation current bigger than the maximum current limit $I_{PK_MAX} = 0,588A$. We chose $I_{SAT} = 0,8A$ leading to a necessary energy storage of:

$$E \geq \frac{L_{MIN} * I_{SAT}^2}{2} \quad (1.2)$$

$$E \geq 627,2\mu J.$$

The maximum tapped inductor turn ratio is determined by the tapped buck converter transfer function (equation 1.3), where D is the maximum duty cycle and N is the tapped inductor turn ratio (equation 1.4). Solving for

the minimum input voltage and maximum output voltage gives us a maximum turn ratio $N = 5,6$.

$$V_{OUT} = \frac{V_{IN}}{\left(\frac{N+1}{D}\right) - N} \quad (1.3)$$

$$N = \frac{N1}{N2} \quad (1.4)$$

The most serious problem for the tapped-inductor buck converter is the leakage energy. It is not possible to achieve perfect coupling between windings, so leakage inductance exists in the circuit. Ideally, the voltage stress of the switching device is:

$$V_{DS_PEAK} = V_{IN} + \frac{N1}{N2} * V_{OUT} \quad (1.5)$$

But in reality, when the switch is turned off, the current in the leakage inductance of winding N2 cannot be reflected to winding N1, so it continuously goes through the drain-to-source capacitor of the MOSFET. All of the energy stored in the leakage inductance will be transferred to this small capacitance, causing a huge voltage spike. This voltage spike can be much higher than the value calculated. This not only increases the switching loss, but can also destroy the switch [7].

To clamp the leakage inductance spike, RC or RCDZ snubbers have been traditionally used in low-cost power supplies. Instead of dissipating this energy in a resistor or in a Zenner diode, we chose to recycle it. The lossless snubber employed provides voltage spike clamping and returns the leakage inductance energy to the output. This implementation [8] works as follows: during MOSFET turn-on period, the steady-state voltage across the clamp capacitor C4 is:

$$V_{C40} = \frac{(V_{IN} - V_{OUT}) * N2}{N1 + N2} + V_{OUT} \quad (1.6)$$

When the MOSFET is turned off, the current in the leakage inductor will go through C4 and D1 so that the leakage inductor energy will be stored in clamp capacitor C4. If C4 is large enough, the increased voltage across C4 is relatively small and the value is about:

$$\Delta V_{C4} = \frac{L_{LEAKAGE} * I_{OFF}^2}{2 * C4 * V_{C40}} \quad (1.7)$$

As a result, the turn-off voltage stress across the internal TinySwitch II MOSFET is effectively clamped as:

$$V_{DS_PEAK} = V_{IN} + V_{C40} + \Delta V_{C4} \quad (1.8)$$

When the MOSFET is turned on, the extra energy stored in the clamp capacitor will be discharged to the

output through diode D2 and winding N2. The voltage across C4 will go back to V_{C40} , the steady-state value. Therefore, all the leakage energy is totally recovered to the output. The currents through D1 and D2 are narrow pulse currents related to the leakage energy, so these can be small. We chose MUR160 1A 600V 35ns ultrafast diodes.

The correct operation of this clamp circuit requires that the voltage across winding N1 is smaller than the steady-state clamp capacitor voltage V_{C40} and this imposes a limitation on the maximum turn ratio:

$$\frac{N1}{N2} \leq \sqrt{\frac{V_{IN}}{V_{OUT}}} \quad (1.9)$$

Solving the equation for minimum input voltage and maximum output voltage yields a value of 2,258. This is smaller than the maximum value necessary to obtain output voltage regulation (equation 1.3). The catch diode voltage stress is a strong function of tapped inductor turns ratio:

$$V_{D3_PEAK} = V_{C40} + \Delta V_{C4} \quad (1.10)$$

This dependency is shown in Fig. 2 below.

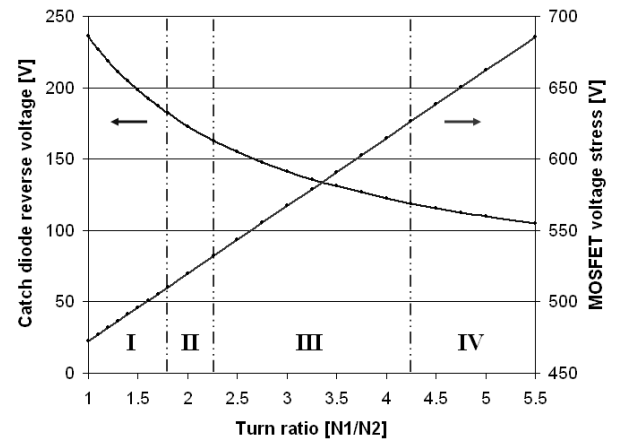


Fig. 2. Main switch and catch diode voltage stress as a function of turns ratio ($V_{IN}=425V$)

There are four sections delimited on the graph:

- I – turn ratios in this range prevent the use of Schottky catch diodes because of increased reverse voltage stress;
- II – turn ratios in this range optimize the snubber operation;
- III – turn ratios in this range decrease catch diode voltage stress at the expense of larger snubber currents and larger voltage stress on the main MOSFET;
- IV – turn ratios in this range should be avoided as the voltage stress approaches the breakdown voltage of the main switch.

A value of 2,2 has been chosen, which optimizes all the design parameters and allows the use of a Schottky diode for increased efficiency. We selected a MBR20200CT double diode for its low forward voltage, negligible switching losses and 200V capability. The selected turn ratio would subject the catch diode to a steady-state maximum of $V_{C40} = 165V$, leaving ample room for clamp capacitor voltage increase ($\Delta V_{C4} \leq 35V$).

Estimating the coupling coefficient for the tapped inductor windings at 0,95, we can use equation (1.7) to calculate the minimum clamp capacitor value. The result is 300pF, which was adjusted to 560pF during prototype testing.

This diode will also be subjected to the primary current reflected to the secondary by the turns ratio:

$$I_{D3_PEAK} = I_{PK_MAX} * \frac{N1}{N2} \quad (1.11)$$

$$I_{D3_PEAK} = 1,3A$$

The complete circuit schematic is shown in Fig. 3.

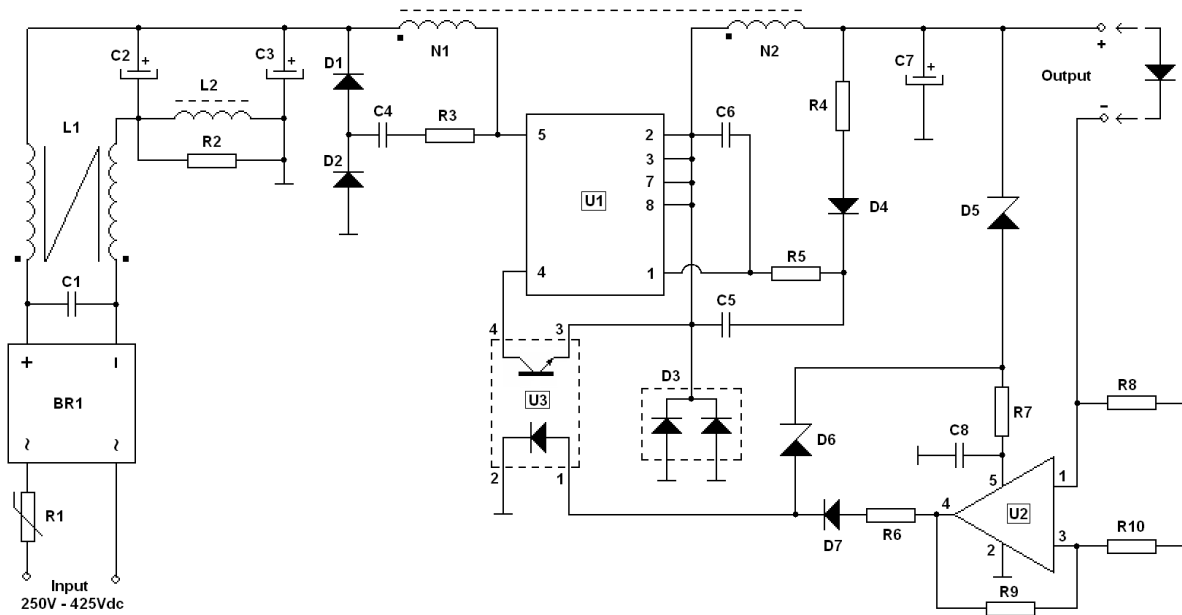


Fig. 3. Proposed driver schematic

Components: U1=TNY268, U2=LM321, U3=LTV356T-D, BR1= DF08S, D1=ES1J, D2=MUR160, D3=MBR20200CT, D4=ES1G, D5=TZMC15-GS08, D6=BZX55C27 (*see text), D7=1N4148, R1=5Ω/1A NTC, R2=1kΩ, R3=10Ω, R4=47Ω, R5=18kΩ, R6=82Ω, R7=100Ω, R8, R9, R10 = (*see text), C1=100nF/500V, C2=C3=10μF/450V, C4=560pF/2kV, C5=1μF/50V, C6=C8=120nF/25V, C7=470μF/50V Low-ESR, L1=CMJ-2-472, L2=100μH/0,2A

The output capacitor (C7) is chosen to minimize output current ripple (<5%); it also needs to have a low ESR because the current pulses have a larger RMS value compared to a conventional buck converter. We selected a SAMXON GT 470μF/50V, 1690mA, 43mΩ capacitor for this position. It has an estimated life of 28000hours@85°C and should provide adequate reliability.

Resistor R1 has a negative temperature coefficient and provides inrush current limiting at powering up. Diode bridge BR1 prevents reverse biasing of the driver in the event of incorrect connection of the input terminals; the loss induced by it is not significant but for maximum performance it should be left out.

The input EMI filter is comprised of C1, L1, C2, L2, R2 and C3. It should be noted that the electrolytic capacitors serve as local energy reservoirs to prevent the driver harmonics from entering the DC bus. L1 provides

common mode rejection, while L2 offers differential mode rejection; R2 prevents peaks in the conducted input spectrum by damping the self resonant frequency of inductor L2.

D1, D2, C4 and R3 are part of the lossless clamp circuit; R3 is necessary to limit the current peaks through the diodes and at the same time it minimizes the EMI signature of the driver.

The TNY268 includes a switched high voltage current source for powering the small signal stages and a 6,3V clamp diode connected between the BP and S pins. To minimize control circuit power consumption, this current source can be disabled by externally supplying the necessary current. This improves light load efficiency and lowers power dissipation in the TinySwitch. The auxiliary supply operation is explained below.

When the internal MOSFET turns off, the dot end of N2 goes negative and D3 conducts; at this same time the no-dot end is positive and charges capacitor C5 to the peak output voltage through R4 and D4. This capacitor has a medium value (1 μ F) and holds its charge for several switching cycles. Because it is referenced to the Source terminals, it is acting as a bootstrap voltage source and can supply current to the BP pin through R5 even when switching cycles are being skipped. Resistor R5 limits the current supplied to 750 μ A, which is sufficient to disable the internal TinySwitch II current source. When the MOSFET turns on, diode D4 prevents reverse biasing of C5; local supply bypass capacitor C6 provides the peak currents necessary for optimum operation of the small signal stages [6]. This allows us to reduce control circuit power consumption by up to 185mW at high input bus voltage, providing a useful improvement in low-load efficiency.

Load current regulation is achieved by sensing the voltage across R8. Instead of using this voltage directly to drive the optocoupler diode, which could impose a significant loss at low output voltages, U2 was employed. The LM321 is a low-power, single-rail operational amplifier that accepts input voltages at ground potential. It is designed to amplify the voltage across R8 to an acceptable level and drives the optocoupler. By minimizing the voltage lost for current sensing, efficiency is further improved by as much as 6% (at an output voltage of 19V). R9 and R10 set the current sense gain; in conjunction with the value of R8 these provide output current selection :

$$\frac{R9}{R10} = \frac{V_{LED_U3} + V_{D7}}{R8 * I_{OUT}} - 1 \quad (1.12)$$

The current tolerance is determined by these three 1% resistors. Ambient temperature also has a very small influence on the output current. The temperature dependency could be eliminated by employing a temperature compensated voltage reference but this increases circuit complexity and cost. Also it is questionable if a higher absolute accuracy is necessary. The values used for different output currents are shown in Table1.

Table 1. Current amplifier component values

Output current [mA]	R8 [Ω]	R9 [k Ω]	R10 [k Ω]
250	0.22	34.8	1
350	0.22	24.9	1
500	0.1	39.2	1
700	0.1	27.4	1

R7 and C8 provide local filtering and decoupling for U2. D5 protects the amplifier from excessive output voltage, as it is only specified to a 32V maximum supply

voltage. Overvoltage protection is provided by D5 and D6; the overvoltage threshold is defined by:

$$V_{OVP} = V_{D5} + V_{D6} + V_{LED_U3} \quad (1.13)$$

To prevent the current regulation circuitry from interfering with the overvoltage protection, D7 and R6 were added. Table 2 presents overvoltage thresholds for the LED arrays tested.

Table 2. LED arrays tested with the proposed driver and the respective overvoltage protection (OVP) thresholds

LED Array type	Nominal voltage [V]	OVP threshold [V]	D6 voltage [V]
BRIDGELUX BXRA-27E0540	18.1	21.1	5.1
BRIDGELUX BXRA-30G0800	21.0	24.2	8.2
BRIDGELUX BXRC-27G1000	27.5	31	15
BRIDGELUX BXRA-40E0810	28.1	32	16
BRIDGELUX BXRA-30G1200	30.0	34	18
LUMILEDS L XK8-PW40	31.5	36	20
BRIDGELUX BXRC27H2000	33.7	36	20
CREE XLamp CXA2520	37.0	40	24
BRIDGELUX - BXRA-27E2000	37.4	40	24
CREE CXA1512	38.0	43	27
CREE CXA1507	38.4	43	27

4. Practical implementation. Tapped inductor fabrication

Based on energy storage needs and estimated losses we selected an EE28/11/11-3F3 core; it provides 2400 μ J of energy storage with an air gap of 0,4mm [9,10]. In this case the A_L value is 295 nH/turn². A smaller core could have been chosen at the cost of increased core losses. The total number of turns can be calculated as follows:

$$N1 + N2 = \sqrt{\frac{L_{MIN}}{A_L}} \quad (1.14)$$

which leads us to $N1 = 58$ turns and $N2 = 26$ turns. The windings are interleaved to improve the coupling and reduce the leakage inductance as much as possible (Fig. 4).

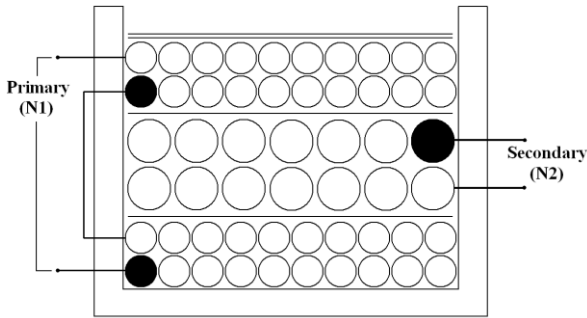


Fig. 4. Tapped inductor construction

The primary is wound with AWG25 wire (0.45mm diameter) in 4 layers; the secondary is wound with AWG22 wire (0.64mm diameter) in 2 layers sandwiched between the primary halves. 0,05mm insulating tape is used between the different sections in an attempt to minimize interwinding capacitance. The finished inductor is shown below along with the measured parameters.



Fig. 5. Finished tapped inductor

Table 3. Finished inductor measured parameters

Parameter	Measured	Calculated or estimated
L1 [μ H]	969	992
L2 [μ H]	196	200
L1+L2 [μ H]	2034	2081
L _{LEAKAGE} [μ H]	58	104
L _{LEAKAGE} [%]	2.84	5 (estimated)
R _{DC} 1 [m Ω]	390	-
R _{DC} 2 [m Ω]	87	-
I _{SAT} [A]	1.46	1.52

The printed circuit board design makes extensive use of surface mounted devices (57%) to reduce as much as possible the converter footprint. Trace length is kept to a minimum, avoiding the introduction of significant parasitic inductances. Traces connecting the input filter capacitors to the rest of the circuit are organized in a star

fashion, forcing harmonic currents to flow through these components and increasing the filter efficacy.

For cooling the TinySwitch, a copper area of 304mm² is connected to the Source terminals. This provides an estimated Junction-Air thermal resistance of 43K/W [11]. The other parts do not require heatsinks due to their low losses.

5. The prototype. Measurements

The prototype used for measurements is shown in Figure 6. Overall dimensions are 61mm*45mm*30mm.

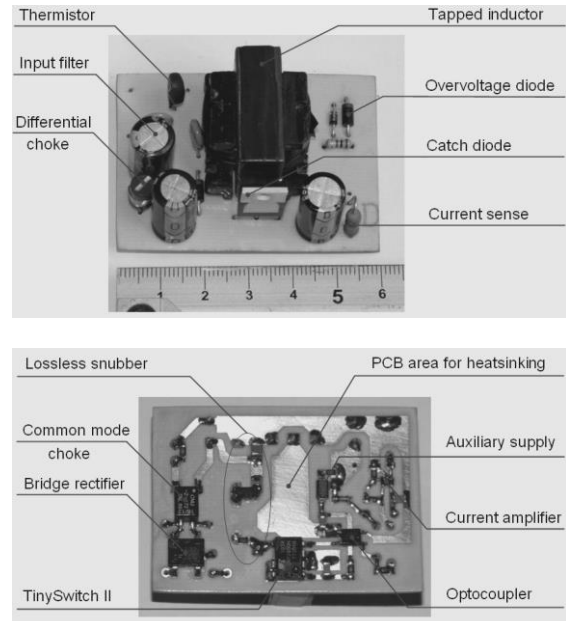


Fig. 6. The converter prototype

The efficiency of the prototype was measured at 4 values of output current, usually employed by LED drivers (250mA, 350mA, 500mA and 700mA) for 4 different types of LED arrays, each having a different operating voltage. The results are presented below ($T_a = 25^\circ\text{C}$).

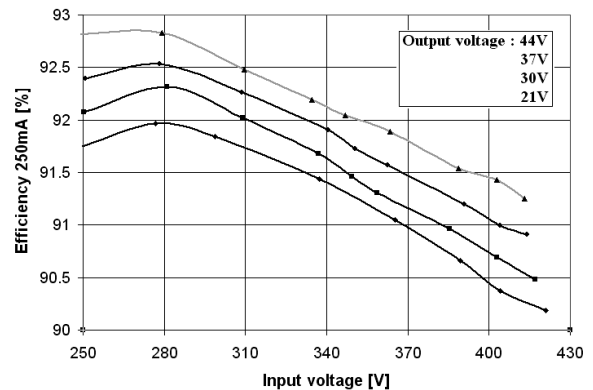


Fig. 7. Efficiency measurements at 250mA output current

Considering the case of a 250mA load (Fig. 7), the efficiency has a minimum of 90,2% for 420V input and 21V output due to the various improvements. The peak efficiency of 92,8% is observed for input voltages around 250-280V. Also the efficiency increases with converter output voltage.

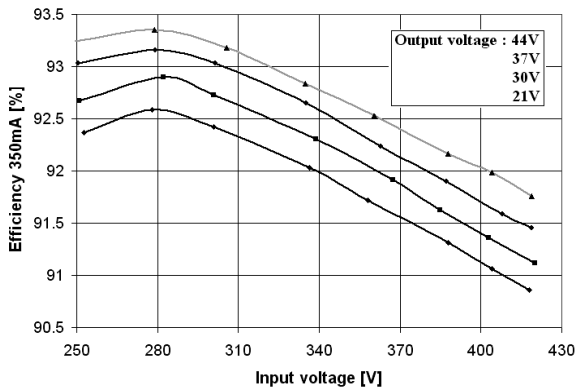


Fig. 8. Efficiency measurements at 350mA output current

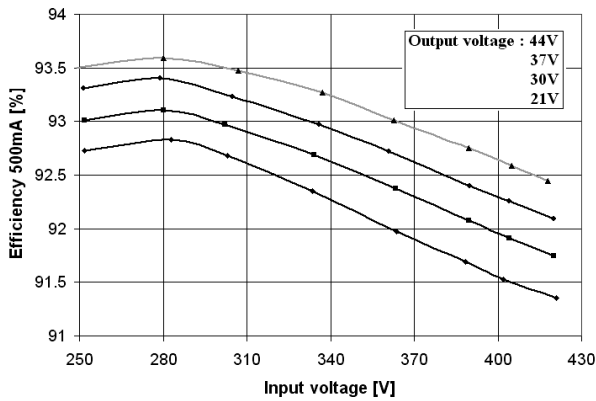


Fig. 9. Efficiency measurements at 500mA output current

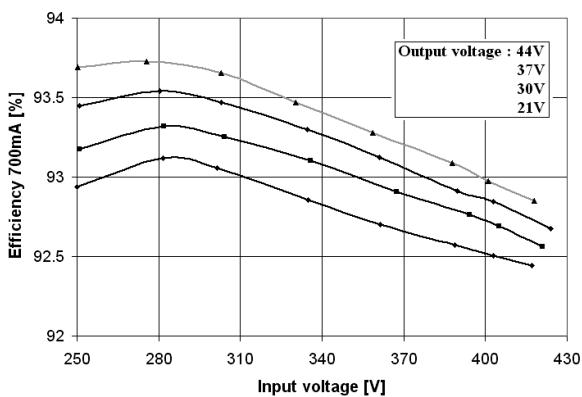


Fig. 10. Efficiency measurements at 700mA output current

Measurements at higher output currents show efficiency improvements over the 250mA case (Figures 8, 9, 10). This is explained by the fact that not all of the converter losses are proportional to the output power. For example control circuit power consumption, MOSFET drain capacitor power, current sense amplifier and current sense resistor power dissipation remain largely unaffected by output conditions. Also the core loss in the tapped inductor and the catch diode conduction loss vary in a nonlinear way relative to the output power. The decrease in efficiency at high input voltages is thought to be due to increased switching losses in the TinySwitch II. Load regulation is normalized to a 21V output voltage for different output currents and it is shown in Figure 11. The deviation is lower than $\pm 0.6\%$ over the whole output voltage range. The driver was also tested at an ambient temperature of 50°C and showed a 3.8% reduction in normalized output current value.

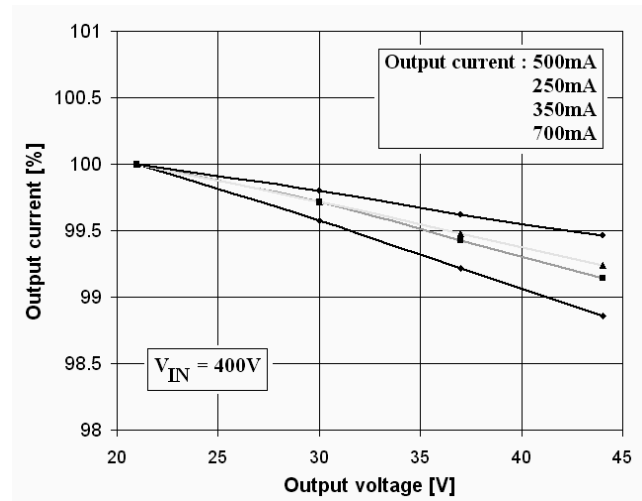


Fig. 11. Driver load regulation

For the no-load graph in Figure 12 the driver was operated in the overvoltage protection mode at the highest input voltage. The power consumption is below 210mW even at high output voltage. A part of this power consumption is due to the current amplifier (which has an almost constant supply current of 450 μ A), TinySwitch II small signal stages (with a supply current of 750 μ A at 19V output voltage and climbing to 2.4mA at 49V output voltage); the remaining power consumption is due to drain capacitance power and other losses.

By replacing resistor R5 with a constant current source, supplying the necessary 750 μ A control current even at high output voltages the no-load power consumption could be further reduced by 77mW, a small benefit for the added cost and complexity.

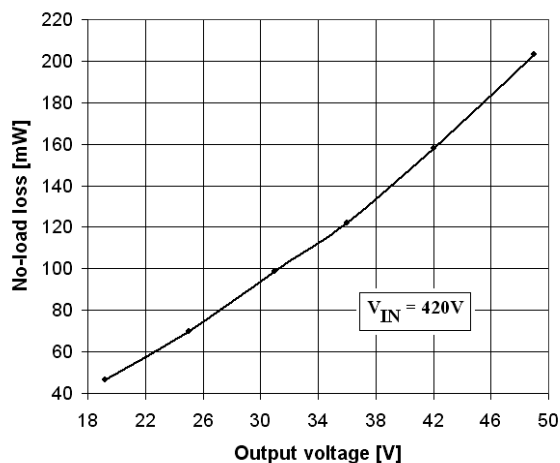


Fig. 12. No-load driver power consumption

6. Conclusion

We designed, fabricated and demonstrated the performance of a new 30Watt driver using low-cost, widely available components. Efficiency figures above 90.2% are easily achieved, with a peak efficiency of 93.8%. The driver is flexible concerning output voltage/current limits and was tested with many types of LED arrays. By optimizing various design parameters the power consumption is reduced to a minimum, the leakage inductance energy is recycled to the output bus and the total system efficacy is increased. The proposed converter has a small footprint (61mm*45mm*30mm), uses only 33 components and includes protections against overvoltage, output short-circuit and over-temperature, providing a good long-term reliability.

References

[1] Solid state lighting and development, US Department of energy, April 2013

- [2] Key trends in the development of LED lighting technology, Jessie Lin, DIGITIMES Research, Taipei, April 3, 2012
- [3] Philips creates the world's most energy-efficient warm white LED lamp, Royal Philips Electronics News Release, April 11, 2013
- [4] Trends in LED Backlighting and Drivers for Mobile Devices and TVs, Publitek European Editors, November 20, 2012
- [5] Adrian Georgescu, Marius Apetrei, Victor Ciupinã, J. Optoelectron. Adv. Mater. **15**(1-2), 37 (2013).
- [6] TNY264-266/268 Datasheet, Revision B, Power Integrations Inc, July 2001
- [7] High-Frequency and High-Performance VRM Design for the Next Generations of Processors, Kaiwei Yao, PhD Dissertation, April 14, 2004
- [8] Tapped-inductor buck converters with a lossless clamp circuit, Yao Kaiwei, Wei Jia, Lee C. Fred, Applied Power Electronics Conference and Exposition, Dallas, Texas, **2**, 693 (2002),
- [9] Applications of Soft ferrites, Philips, October 1, 1998
- [10] Inductor Design Software, Magnetics Inc, <http://www.mag-inc.com/design/software/inductor-design>
- [11] AN-2020 – Thermal Design By Insight, Not Hindsight, Texas Instruments, April 2013
- [12] LEDs Magazine - "A three stage power supply efficiently drives multiple LED strings", May-June 2010;
- [13] High brightness LED driver solutions for general lighting, ON Semiconductor, 2009
- [14] LED Drivers for High-Brightness Lighting, Vol. 1, National Semiconductor, 2011

*Corresponding author: apetrei.marius@gmail.com